J Mater Sci: Mater Med (2010) 21:2035–2047
DOI 10.1007/s10856-010-4074-9

Nucleation and growth of octacalcium phosphate on treated titanium by immersion in a simplified simulated body fluid

Enori Gemelli · Cristiane Xavier Resende · Gloria Dulce de Almeida Soares

Received: 28 July 2008 / Accepted: 26 March 2010 / Published online: 14 April 2010

Abstract A simplified simulated body fluid solution (S-SBF) was used to study the kinetics and mechanism of nucleation and growth of octacalcium phosphate (OCP) on the surfaces of alkali and heat-treated titanium samples. After the alkali and heat treatments, the samples were soaked in S-SBF for periods varying up to 24 h. A thin layer of poorly crystallized calcium titanate was formed after 15 min of immersion, allowing for the deposition of another layer of amorphous calcium phosphate (ACP). After 2.5 h of immersion, OCP nuclei were observed on the surface of the ACP layer. After 5 h of immersion in S-SBF solution, the specimens were completely covered with a homogeneous plate-like layer of OCP. Analyses by transmission electron microscopy revealed that nucleation and growth of OCP occurred concomitantly to the crystallization of ACP in hydroxyapatite (HA). This transformation took place by solid-state diffusion, forming a needle-like HA structure underneath the OCP film.

1 Introduction

Although nucleation of biological apatite has been investigated and discussed for many years, the theory that amorphous calcium phosphate (ACP) and/or octacalcium phosphate (OCP) act as precursor pathways for the biological formation of apatite is not unanimously accepted. In an investigation of early embryonic chicken bone, Wu et al. [1] detected hydrogen phosphates and/or protein phosphoryl groups that might be part of a range of phosphate environments in early mineralization. More recently, Crane et al. [2] used micro-Raman spectroscopy to monitor mineral formation at the suture boundaries of mice calvaria and, by adding FGF2 to the medium, they induced rapid mineralization. Their results revealed the presence of OCP. Octacalcium phosphate has also been identified by other techniques as one of the Ca–P phases that nucleate in the early stage of biomineralization, which is transformed into hydroxyapatite (HA) in biological matrix [3, 4]. Observations of this nature have been used to argue that OCP is present in new bone mineral formation. However, handling of the sample, dehydration, complexity of in vivo environment, structure, nonstoichiometry, impurities and size-related effects are the major factors that affect the nature of the early formed mineral phase.

Many in vitro studies have reported the deposition of OCP and HA films on chemically treated titanium surfaces by soaking the material in simulated body fluid (SBF) solutions [5–8]. Theoretical analyses have shown that HA and OCP are thermodynamically stable phases in SBF solutions at physiological pH and temperature [9]. HA is thermodynamically more stable than OCP, but the nucleation rate of OCP is higher than that of HA in SBF solutions [9–11]. These theoretical studies show that Ca–P precipitation on bioactive materials may lead to the formation of a layer of OCP, followed eventually by the formation of an external layer of HA. Feng et al. [6] chemically activated a titanium surface with NaOH in order to study the deposition mechanism of calcium

E. Gemelli (✉)
Department of Mechanical Engineering, Center of Technological Science, State University of Santa Catarina, Campus Universitário, Bairro Bom Retiro, 631, Joinville 89223-100, SC, Brazil
e-mail: gemelli@joinville.udesc.br

E. Gemelli · C. X. Resende · G. D. de Almeida Soares
Metallurgy and Materials Engineering, Federal University of Rio de Janeiro, COPPE, 68505, Rio de Janeiro 21941-972, RJ, Brazil

phosphate in simple supersaturated calcification solution. In their experiment, two layers of Ca–P crystals were found on the activated titanium surface: OCP deposited from different concentrations of supersaturated calcification solution, followed by HA with [001] preferred orientation on OCP [6]. Many other studies have reported the deposition of OCP and/or HA on bioactive titanium by biomimetic methods [5, 8, 12, 13]. Bioactive titanium surfaces were prepared by chemical treatment in NaOH, nitric acid or modified simulated body fluid solutions, followed by immersion in SBF solutions or supersaturated calcium phosphate solutions. The structure formed on pre-treated titanium surfaces generally depends on the composition of the solution. Subsequent films prepared under physiological conditions exhibited structures composed of OCP and/or HA.

Lu and Leng [14] investigated the formation of Ca–P phases on alkali and heat-treated titanium surfaces, followed by immersion in Kokubo revised SBF (R-SBF) solution. Their study revealed that OCP, instead of HA, nucleated directly from amorphous calcium phosphate. The OCP crystals grew continuously on the titanium surfaces rather than transforming into apatite. Calcium titanate was also identified by electron diffraction as a precursor phase to Ca–P deposition [14]. Similar studies in Kokubo conventional SBF solution lead to a film essentially composed of apatite [7, 15–17]. The difference in structure of the Ca–P layer may be attributed to the difference in the concentration of carbonate ions in the solutions [9].

Recently, Kamakura et al. [18] confirmed that OCP is more resorbable and enhances bone formation more than do other Ca–P phases such as β-tricalcium phosphate (β-TCP) and HA. Also, it was found that the OCP phase grows preferentially, even in the presence of β-TCP seeds from solutions supersaturated with β-TCP, HA and OCP [19]. Therefore, presuming that OCP or OCP-like phosphate may be a transient precursor strategy for the initiation of biological apatite, deposition of OCP film may lead to the rapid formation of a biological apatite layer on the surface of the implant. Ca–P films are also well known as the main requirement for biological fixation and long-term clinical success [20, 21]. These films have been successfully deposited on bioactive titanium surfaces by biomimetic processes in SBF solutions. Thus, the purpose of this investigation was to coat pure titanium with OCP by a similar process, using a simplified SBF solution. This solution was already theoretically studied [22] and a film of OCP on alkali and heat-treated titanium surfaces was observed by soaking the material in this solution for one or more days [15]. The aim of this work was to study the initial period of formation of OCP up to 24 h, involving the kinetics and the nucleation and growth mechanism of OCP. This study was also motivated by the fact that the solution used herein leads to the formation of an OCP film on the titanium surface instead of a HA film, as reported in many biomimetic studies [5, 6, 13, 23, 24]. Moreover, the nucleation and growth of this OCP film is very fast. To our knowledge, a systematic study of such rapid film formation using a simplified solution with calcium and phosphate concentration equal to SBF has not yet been reported.

2 Materials and methods

2.1 Preparation of simplified simulated body fluid solution (S-SBF)

The simplified solution (S-SBF), which was designed by Resende et al. [15] in their quest for a less complex composition, consists of sodium bicarbonate (99.7% pure), dipotassium hydrogen phosphate (99% pure) and calcium chloride (96% pure). All reagents were from VETEC Química Fina, Brazil. The impurities present in the precursor reagents were specified by the company. The preparation consists of sequentially dissolving reagent-grade $NaHCO_3$, $K_2HPO_4{\cdot}3H_2O$ and $CaCl_2$ in distilled water at approximately 36.5°C buffered to pH = 7.4 with Tris-hydroxymethyl aminomethane (TRIS) and HCl, according to the guidelines set forth in the ISO 23317: 2007 standard. Table 1 shows the ionic concentration of the S-SBF solution compared with that of human blood plasma.

2.2 Sample preparation and analyses

Commercially pure 8 × 8 × 1 mm titanium sheets were polished mechanically using Si carbide sandpaper from grade 100, 240, 400–600 grits. The samples were ultrasonically cleaned in acetone, alcohol and distilled water for 10 min each, followed by immersion in 5 M NaOH (VETEC Química Fina, Brazil) aqueous solution at 60°C for 24 h, then washed with distilled water, dried at 50°C in air and heated at 600°C for 1 h in a furnace. After cooling

Table 1 Composition of S-SBF solution and of human blood plasma (mM)

	Na^+	K^+	Ca^{2+}	Mg^{2+}	Cl^-	HCO_3^-	HPO_4^{2-}	SO_4^{2-}
Plasma	142.0	3.6–5.5	2.12–2.6	1.0	95–107	27.0	1.0	0.65–1.45
S–SBF	4.2	2.0	2.5	–	5.0	4.2	1.0	–

to room temperature, each Ti sheet was soaked in 16 ml of S-SBF solution at 37°C for various periods (15–30 min, from 1 to 24 h), removed from the S-SBF, washed with distilled water and dried in air atmosphere. The samples immersed in this solution were maintained leaning and its superior side was analyzed.

Sample surfaces were analyzed by scanning electron microscopy (SEM), X-ray diffraction (XRD), X-ray photoelectron spectroscopy (XPS), and transmission electron microscopy (TEM) coupled to X-ray energy dispersive spectrometry (EDS). The SEM analyses were carried out under a JEOL JSM 6460LV microscope (Japan) operating between 10 and 20 kV. A Shimadzu XRD-6000 X-ray diffractometer (Japan) was used to identify the phases formed on titanium surfaces. A CuK_{α} radiation source was used and the incidence beam scan was 2°/min. The XRD patterns were recorded with scan range from 3 to 60° (2θ), incremental steps of 0.02° and a count time of 0.6 s. The XPS analyses were performed with a Phoibos 100 spectrometer (SPECS, Germany). The X-ray source was generated by MgKα (1253.6 eV), with 200 W power. The C1 s peak (284.6 eV) was used as an internal standard to correct the peak shifts caused by the accumulation of surface charge on insulating samples. In preparation for the TEM analysis, the samples were immersed in an ethanol bath with ultrasonic vibration to separate the layer of coating from the titanium substrate. The material was deposited on a TEM copper grid coated with formvar and carbon films and examined in a JEOL 2000FX microscope (Japan) operating at 200 kV. This analysis was performed on particles extracted from the coatings produced by immersion in S-SBF for 1, 2.5 and 6 h.

3 Results and discussion

3.1 Alkali and thermal treatments

Figure 1 shows the morphology of the titanium surface after alkali and thermal treatments. Note the network structure with high interpenetrating sub-micrometric porosity due to the attack of NaOH. The XPS results depicted in Fig. 2 indicate that the main components of this sample surface were Ti, O, and Na, with small amounts of C (due to contamination by XPS), Ba and Si. Peaks associated with Ba and Si may arise due to impurities in the reagents used to treat Ti or prepare the S-SBF. Sodium (Na) was found in its monovalent state (Na^{+}) with a binding energy of 1071.21 eV (Fig. 2b), which is low energy compared with that of pure Na 1 s (1072.00 eV). The chemical shift indicated that the sodium (Na) was bound to other chemical species such as Ti and oxygen. The binding energies of O 1 s (Fig. 2c) indicated that the

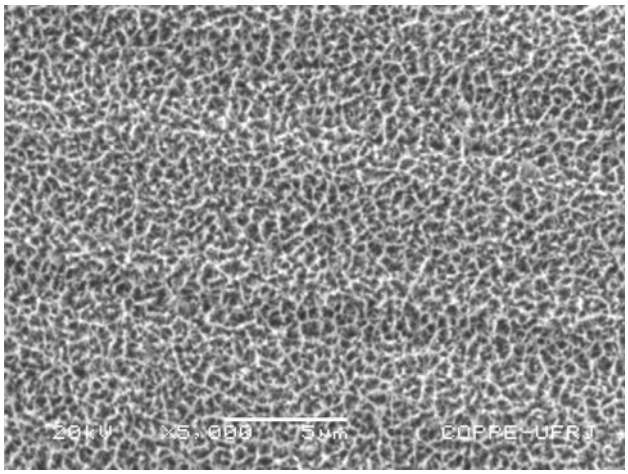

Fig. 1 SEM micrograph of titanium surface treated in 5 M NaOH aqueous solution at 60°C for 24 h and sequentially heat-treated in air at 600°C for 1 h

surface contained titanium and barium oxides and hydroxyl, most likely from Ti–OH groups formed by the reaction between the Ti substrate and OH^{-} ions in the solution. Figure 2d presents the Ti 2p spectrum, together with the oxidation states. Three oxidation states are presented: Ti^{0}, Ti^{3+} and Ti^{4+}. Ti^{0} corresponds to metallic Ti and was detected by XPS because of the high porosity produced by the alkali attack on the titanium surface. The Ti^{4+} peak originates from TiO_2 and sodium titanate oxide and the Ti^{3+} peak indicates the presence of Ti_2O_3 and/or barium sodium titanate oxide.

It is well known that when metallic titanium is exposed to ambient air at room temperature, a passive oxide film forms spontaneously on its surface. This passive film is amorphous, very thin (5–10 nm thickness) [25], and composed of three layers [26, 27]: the first layer adjacent to metallic titanium is TiO, the intermediary layer is Ti_2O_3, and the third and most important layer in thickness, which is in contact with the environment, is anatase TiO_2. During the alkali treatment, OH^{-} ions react with this passive oxide film, forming titanate hydroxide. These hydroxides are essentially joined by Na^{+} ions in the aqueous solution, resulting in the formation of a porous network layer of sodium titanate hydroxide [23]. Some titanate hydroxide may be also joined by barium, forming barium sodium titanate hydroxide. Titanate hydroxide not bonded with Na^{+} (and eventually with Ba^{+}) is converted into TiO_2 by dehydration during heating. After the heat treatment, amorphous sodium titanate and/or sodium titanate oxide is formed by removal of water from the sodium titanate hydrogel layer.

Figure 3a shows broad low peaks ascribed to sodium titanate oxide at approximately $2\theta = 24.5$ and 48.8°. The broad peaks indicate low crystallinity, i.e., a 1 h heat

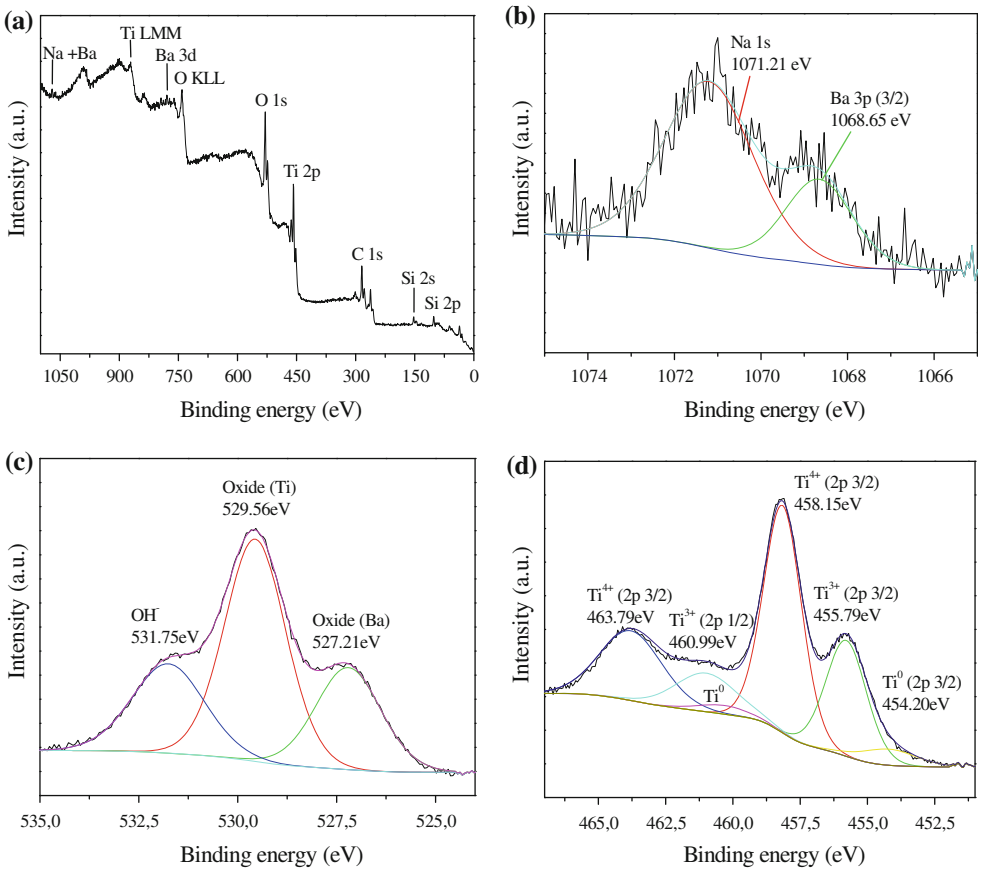

Fig. 2 XPS binding energy of titanium after surface modification with alkali and heat treatments: XPS surface survey scan (**a**), high-resolution scan spectra of Na 1 s (**b**), O 1 s (**c**) and Ti 2p (**d**)

treatment at 600°C does not suffice to ensure total transformation of the sodium titanate hydrogel layer, which can be identified by a hump at the left side of the XRD pattern of titanium (near $2\theta = 10°$) that has undergone alkali treatment but not been heat-treated (Fig. 3b). Many studies have reported that heat treatments transform sodium titanate hydrogel layers into amorphous sodium titanate layers [13, 16, 23, 28]. The present study demonstrates that the sodium titanate hydrogel layer can be partially crystallized by a 1 h heat treatment at 600°C (Fig. 3a). Many studies have failed to find sodium titanate peaks by XRD after heat treatments at 600°C for 1 h [13, 23, 28]. This finding has led to the suggestion that sodium titanate hydrogel layers formed by alkali treatments stabilize as amorphous sodium titanate layers after a 1 h heat treatment at 600°C. Nevertheless, these discrepancies may be attributed to the conditions of alkali treatment, and possibly also to the XRD technique employed and to the preparation of the titanium surface, which may influence the NaOH reaction kinetics. Consequently, the layer may be thicker or thinner, and thus more visible or less visible by XRD. Li et al. [7] demonstrated the formation of large amounts of crystalline $Na_2Ti_6O_{13}$ phase on a titanium alloy immersed in 10 M NaOH at 60°C for 24 h, and then heat-treated in air at 600°C for 1 h. This thermal treatment was also performed

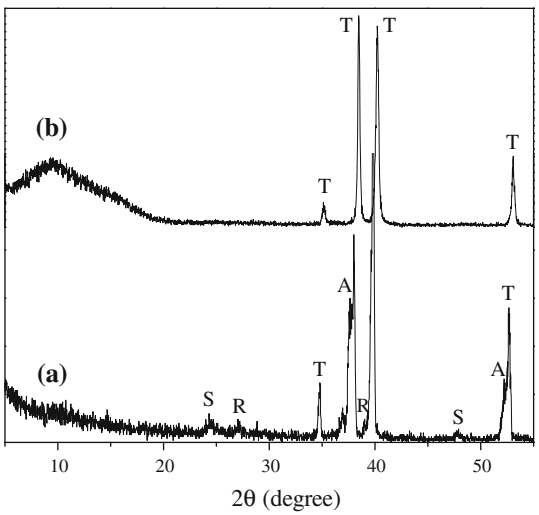

Fig. 3 XRD patterns of titanium treated in 5 M NaOH aqueous solution at 60°C for 24 h and heated in air at 600°C for 1 h (*a*), and of titanium treated in 5 M NaOH aqueous solution at 60°C for 24 h (*b*). *T* titanium, *S* sodium titanate, *A* anatase and *R* rutile

on titanium samples after immersion in 5 and 10 M NaOH aqueous solutions at 60°C for 24 h [29]. Using XRD, sodium titanate peaks were identified as $Na_2Ti_5O_{11}$ in all the samples [29]. In the current investigation, the

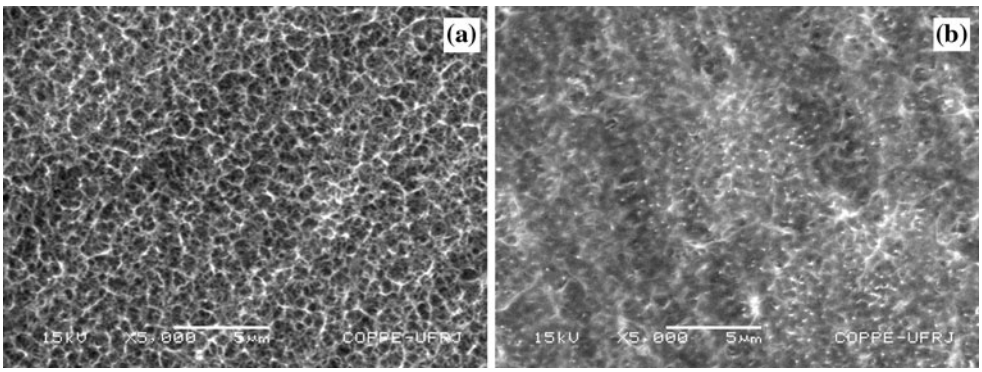

Fig. 4 SEM micrographs of alkali and heat-treated titanium surfaces after immersion in S-SBF for 15 min (**a**), and 1 h (**b**)

crystalline part of sodium titanate that appears in Fig. 3a is best matched to $Na_2Ti_6O_{13}$ (JCPDS 73-1398 card).

Crystalline rutile and anatase (TiO_2) were also detected by XRD (Fig. 3a). After the alkali treatment, the samples were exposed to ambient air at room temperature and washed with water. This procedure led to the formation of a passive oxide film at the interface with the metal due to the porosity of sodium titanate. During heating, the passive film is transformed into crystalline rutile and anatase. Therefore, the Ti^{4+} found in the spectra of O 1 s (Fig. 2c) and Ti 2p (Fig. 2d) also originates from the oxide formed in contact with the metal. The Ti^{3+} peak in the Ti 2p spectrum (Fig. 2d) may originate from Ti_2O_3 passive film not converted into crystalline TiO_2. However, the fact that TiO was not identified by XPS suggests that all the passive film was crystallized and that the Ti^{3+} comes from barium sodium titanate oxide in the form of $BaNaTiO_3$, which was formed by the removal of water from the barium sodium titanate hydroxide during heating. Because oxygen can penetrate porous sodium titanate, diffusion of titanium and/or oxygen through the oxide film in contact with the substrate occurs during heating, increasing the thickness of rutile and anatase film.

3.2 Initial period of the coating process (from 15 min to 2.5 h)

Various coatings were produced on alkali and heat-treated titanium by controlling the immersion time. It was found that calcium deposition occurred before phosphate deposition when treated titanium was soaked in supersaturated S-SBF solution. Figure 4a, b are SEM photographs of treated titanium surfaces after immersion in S-SBF for 15 min and 1 h, respectively. No obvious morphological changes were visible in the microporous structure of sodium titanate after immersion in S-SBF for 15 min (Fig. 4a). Increasing the immersion time in S-SBF to 1 h led to the deposition of a new gel-like layer on the porous structure of sodium titanate (Fig. 4b). No new peaks were

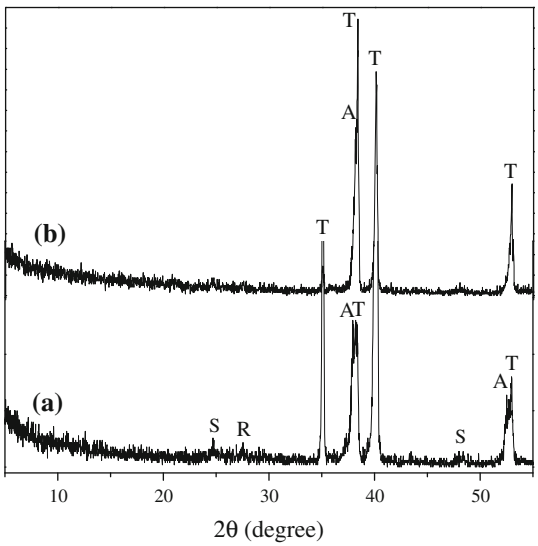

Fig. 5 XRD patterns of alkali and heat-treated titanium surfaces after immersion in S-SBF solution for 15 min (*a*), and 1 h (*b*). *T* titanium, *S* sodium titanate, *A* anatase and *R* rutile

detected by XRD in these samples, indicating that the new layers could be amorphous and/or very thin (Fig. 5). In Fig. 5b, rutile (*R*) and sodium titanate (*S*) are no longer discernable on the XRD spectra because of the deposit formed during the immersion in S-SBF solution. The XPS analysis of the sample soaked in S-SBF for 15 min revealed the deposition of calcium from solution (Fig. 6). No phosphor was found, indicating that the surface was probably composed of a calcium titanate film on a sodium titanate phase. The calcium titanate film must have been very thin, since the sodium (and barium) peaks were visible. Moreover, the binding energies of O 1 s and Ti 2p were consistent with those of TiO_2 and sodium titanate phases in the sodium titanate layer. The Ti 2p spectrum in Fig. 6d indicates that the binding energy of approximately 4,562 eV corresponded to $CaTiO_3$ and/or $BaNaTiO_3$. The composition of the specimen immersed in S-SBF for 1 h was also evaluated by XPS and the results indicated that

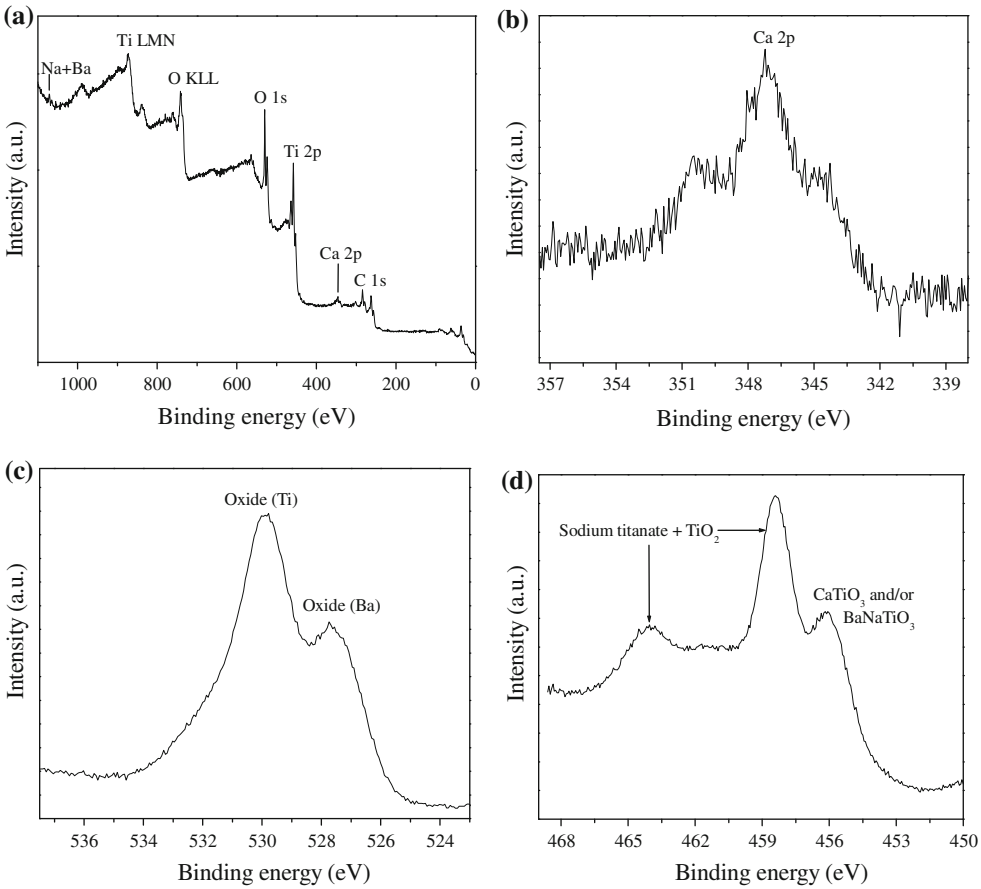

Fig. 6 XPS spectra of treated titanium after immersion in S-SBF solution for 15 min. XPS surface survey scan (**a**), and spectra of Ca 2p (**b**), O 1 s (**c**) and Ti 2p (**d**)

the gel-like layer was composed mainly of phosphor, calcium and oxygen (spectrum not shown here).

The structure of the coating produced on the alkali and heat-treated titanium surface after immersion in S-SBF solution for 1 h was also assessed by TEM on the layer of coating detached from the substrate by ultrasound. Figure 7a shows the bright-field TEM image of a region containing particles of amorphous calcium phosphate with islands of a needle-like structure. The electron diffraction pattern (Fig. 7b) confirms the amorphous nature of the gel-like layer of calcium phosphate observed in Fig. 7a. A TEM analysis of particles from the coating produced by immersion in S-SBF for 1–2.5 h also revealed the presence of calcium titanate particles (Fig. 8a, b). The strong Cu peak indicates that the analysis was performed close to the copper grid. Figure 8b also highlights small amounts of sulfur, chloride, phosphor and silicon incorporated into the structure during the deposition process. Figure 8a shows rounded particles of poorly crystallized calcium titanate. Lu and Leng [14] also found this phase on a bioactive titanium surface after immersion in R-SBF solution. However, in this case, the calcium titanate was totally crystallized because the samples were kept in the solution for 1 month (the solution was refreshed every 3 days). The electron diffraction pattern of these crystalline grains was indexed as the diffraction of cubic structure of $CaTiO_3$ [14]. Indications of calcium titanate in vivo were found in recent years on implants of alkali modified plasma-sprayed titanium coatings inserted in dog femur [30]. EDS analyses of the implant one month after implantation revealed the presence of calcium and titanium at the interface between the titanium implant and bone. No phosphor was detected by this technique, indicating that calcium titanate could be formed and could link directly to the bone. In this work, the evidence revealed by XPS and TEM indicated that the porous structure of sodium titanate was covered by a continuous thin film of poorly crystallized calcium titanate. This film, which was formed shortly after the sample's immersion in S-SBF solution, was followed by another thicker film of amorphous calcium phosphate (ACP) formed on the surface during the initial period of formation of the Ca–P coating.

The mechanism of Ca–P coating on alkali and heat-treated titanium in SBF solution was proposed by Kokubo et al. [28]. When exposed to SBF solution, bioactive titanium generally releases the Na^+ ion from its sodium titanate surface into the SBF via exchange with H_3O^+ ions in the fluid, thereby forming many Ti–OH groups on its surface [28]. As a result, the surface is negatively charged, and then reacts with Ca^+ cations in SBF to form a calcium titanate. As the Ca^{2+} cations accumulate, the surface

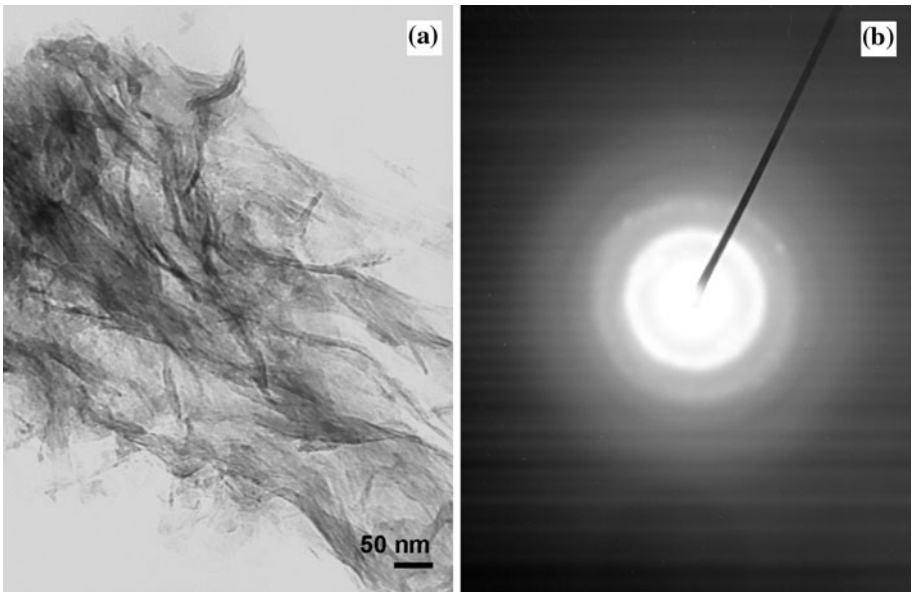

Fig. 7 TEM morphology of needle-like structure surrounded by amorphous calcium phosphate formed on alkali and heat-treated titanium surface after immersion in S-SBF solution for 1 h (**a**), and its corresponding electron diffraction pattern (**b**)

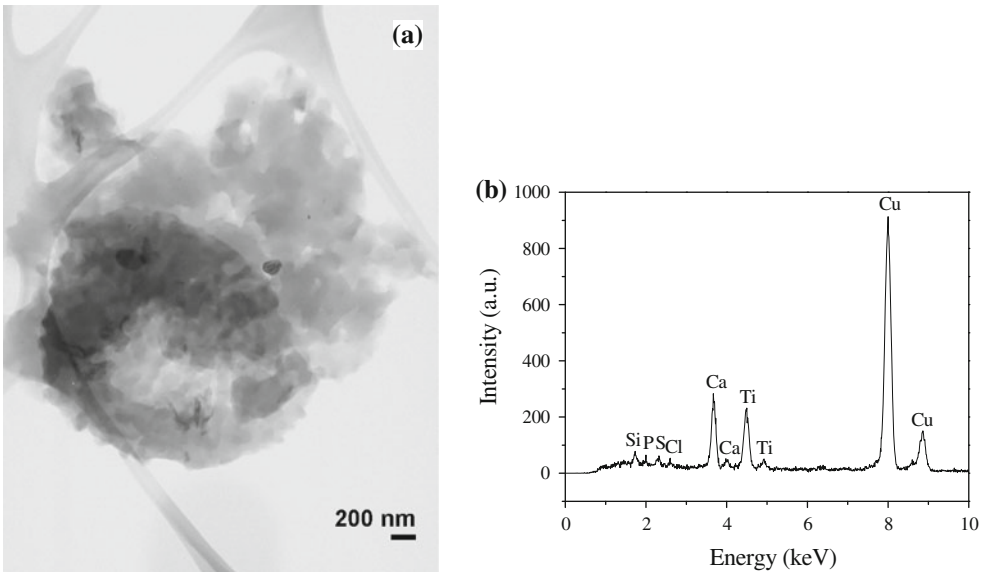

Fig. 8 TEM image (**a**), and its EDS spectrum (**b**) of calcium titanate obtained from the layer of alkali and heat-treated titanium surface after immersion in S-SBF solution for 2.5 h

becomes positively charged, reacting with phosphate anions to form a bone-like apatite [28]. Chen et al. [23] investigated the release of Na^+ ions from NaOH-treated titanium with and without a 1 h heat treatment at 600°C. The specimens were immersed in a buffer solution at biological temperature and pH and the release of Na^+ ions into the buffer solution was measured after 1, 3, 5 and 7 days. They found that the Na^+ concentration increased sharply in the buffer solution, and that the amount of this increase in NaOH heat-treated titanium was higher than in NaOH heat-treated titanium. The Na^+ ion concentration reached its highest dissolution level of 0.20 and 0.55 mM after 1–3 days in samples with and without heat treatment, respectively. The sodium titanate appeared to become more stable after heating, hindering the release of Na^+ ions. This experiment confirmed the dissolution of Na^+ ions in the solution. However, compelling and irrefutable experimental data about its dissolution via exchange with H_3O^+ ions in the fluid has not yet been presented, leaving room for speculation about other mechanisms. For instance, some dissolution due to the chemical potential between solid/liquid phases might suffice to ensure the formation of Ti–OH bonds on the surface. Na^+ ion dissolution, especially from the amorphous sodium titanate part, which is less stable, could occur along with dissolution and redeposition of Ti through the reaction:

$$H_2O + O^{2-} = 2OH^-,$$

creating Ti–OH groups and/or attracting Ca^{2+} from the solution to form a thin layer of calcium titanate. It should be noted that Ti is highly reactive and that the solution is slightly alkaline, facilitating the formation of Ti–OH on the surface.

3.3 Transient stage and last period of the coating process (from 2.5 to 24 h)

The morphology of the initial amorphous calcium phosphate film changed after it was soaked in S-SBF solution for more than 1 h. A uniform and thicker layer of Ca–P with a ribbon-like morphology at its surface was observed after immersion for 2.5 h in S-SBF solution (Fig. 9a). As the soaking time increased, the film became denser and the ribbon-like morphology resembled a platelet network structure (Fig. 9b). Immersion in S-SBF for 5 h yielded a uniform plate-like layer on the surface of titanium samples (Fig. 9c). Nevertheless, the specimens displayed plate-like crystals with well-defined and regular shapes after 10 or more hours of immersion (Fig. 9e–h). This plate-like morphology is compatible with OCP morphology [31, 32]. Indeed, the XRD patterns revealed an OCP peak at $2\theta = 4.7°$ in the samples immersed in S-SBF for 20 and 24 h (Fig. 10). This peak corresponded only to the diffraction pattern of OCP (JCPDS 44-0778 card). The coatings of samples immersed in S-SBF solution from 2.5 to 15 h (Fig. 10) displayed many other peaks. A small peak was already visible at approximately $2\theta = 26°$ after 2.5 h of immersion in S-SBF solution. Due to their structural similarity, this peak may be attributed to OCP and/or HA. Increasing the immersion time gave rise to new OCP/HA peaks, all of increasing intensity, indicating that the coating became increasingly crystalline and/or thick.

Crystalline needle-like structures were observed by TEM on particles from the layer produced in S-SBF for 2.5 h (Fig. 11a). Because the crystalline needles were extremely small, multiple needles were subjected to electron diffraction, yielding results compatible with HA data (Fig. 11b). Indeed, TEM-EDS analyses revealed that the needles had an average Ca/P ratio of approximately 1.7 (Fig. 11c). Moreover, these HA particles seem to grow from the adjacent OCP plate. Needle-like structures were also observed by electrochemical deposition of calcium phosphate on titanium under controlled atmospheres [32] and on bioactive titanium metal soaked in SBF [33]. These structures were identified as HA [32, 33].

The analyses as well the features observed in the high-magnification TEM micrograph and its diffraction pattern confirm that the amorphous calcium phosphate layer was converted into HA as the immersion time in S-SBF increased. The coating goes through a transient stage when the amorphous Ca–P metastable phase is transformed into stable crystalline HA phase. This transformation occurs by solid-state diffusion along with OCP formation, which is ensured by a heterogeneous reaction during the immersion process. It is interesting to note that the weak rings depicted in Fig. 7 correspond to HA, which grew in a needle-like morphology as the immersion time increased, as is clearly visible in Fig. 11.

Figure 12 is a bright-field image and its diffraction pattern of B = 110 of a particle from the coating produced by immersion in S-SBF for 6 h. The morphology displayed in Fig. 12a is typical of a single highly porous crystalline OCP plate. Checking the $d_{(hkl)}$ from the electron diffraction pattern of the single crystal (Fig. 12b), we found that the smallest R resulted in a $d_{(hkl)}$ of approximately 0.94 nm. It is well known that HA does not have any $d_{(hkl)}$ value around 0.9 nm. A value over 0.9 nm is unique to OCP. Therefore, the diffraction pattern in Fig. 12b must be assigned to the diffraction plane of OCP.

It is interesting to compare the electron diffraction results with those of the X-ray diffraction. The XRD spectrum of the coating obtained after 2.5 h of immersion exhibited a small peak at approximately $2\theta = 26°$. This peak was essentially from HA, since nucleation of OCP begins at this immersion time, resulting either in a small amount of OCP or, more likely, in nuclei particles of poorly crystallized OCP. This peak increased sharply with the immersion time as a result of the crystallization of HA and OCP as well as the growth of OCP. The absence of an XRD peak at $2\theta = 4.7°$ in the samples immersed in S-SBF up to 15 h is another interesting point. The SEM micrographs in Fig. 9 reveal that the plate-like OCP crystals grew somewhat perpendicular to the substrate. Preferential growth of OCP is reported by Iijima [34]. Lu and Leng [14] also believe that, in their investigations, preferential growth of OCP on bioactive titanium was responsible for no diffraction of OCP at $2\theta = 4.7°$. Therefore, the absence or low intensity of $2\theta = 4.7°$ in this study may have been due to the preferential growth of OCP along the d-axis ($2\theta = 26°$).

HA is reportedly more thermodynamically stable than OCP in physiological conditions; however, OCP formation is kinetically more favorable than that of HA [9–11, 22]. Note that some researchers have demonstrated that HA nucleates and grows directly from ACP [13, 23, 28, 29] or from OCP [6, 11], or via transformation of OCP into HA [11, 35], while others have reported the growth of OCP directly from ACP in SBF solutions [14, 15, 34, 36]. In the present study, stable OCP crystals were formed in physiological conditions by heterogeneous nucleation. These crystals nucleated on a transient ACP layer and grew continually, regardless of the transformation of ACP into

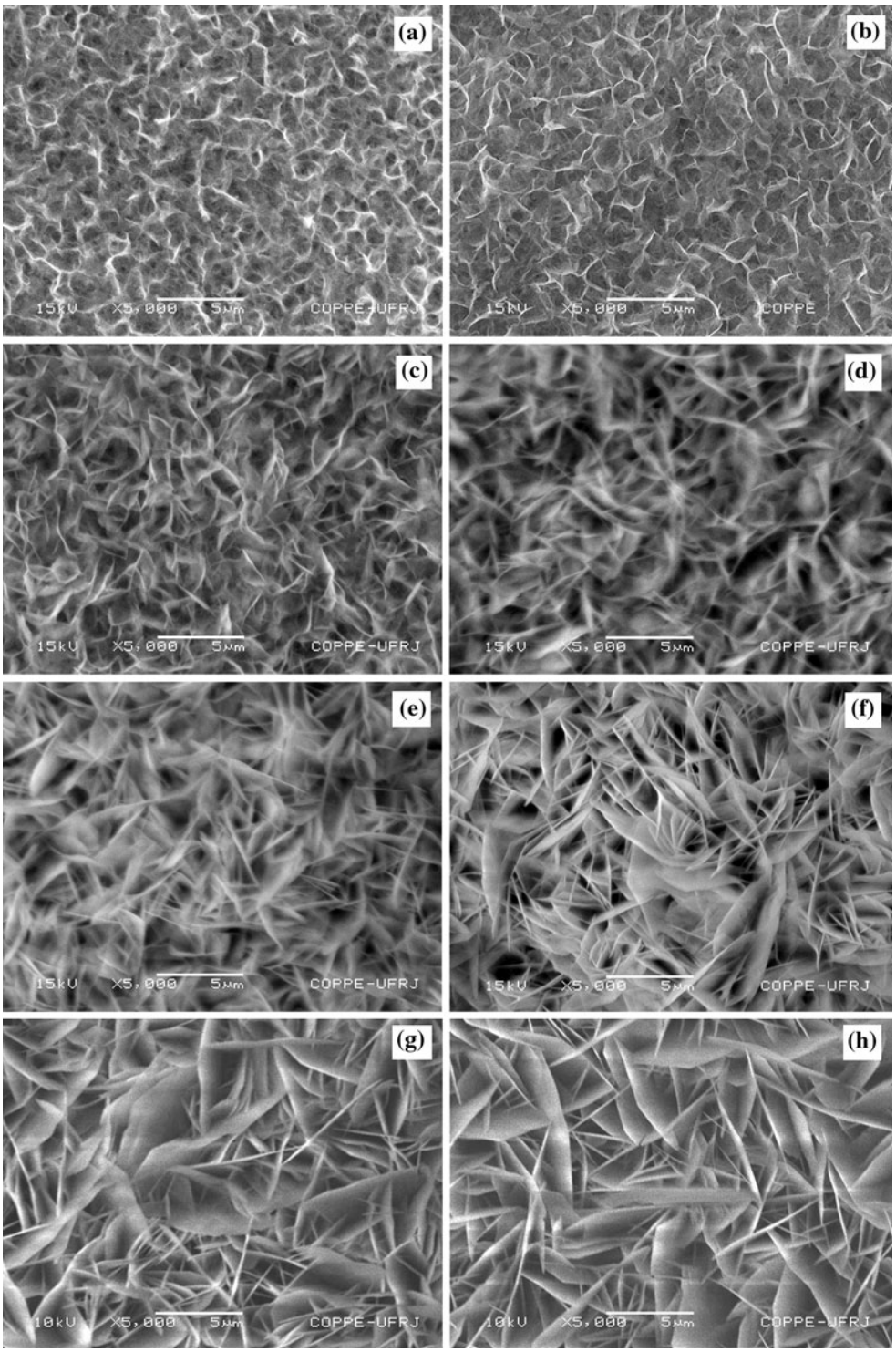

Fig. 9 SEM morphology of the coatings after immersion in S-SBF for 2.5 h (**a**), 3.5 h (**b**), 5 h (**c**), 7.5 h (**d**), 10 h (**e**), 15 h (**f**), 20 h (**g**) and 24 h (**h**)

HA. Lu and Leng [14] argue that OCP can grow without transforming into HA as long as the driving force for OCP growth is greater than that for HA formation. To maintain this driving force, it seems important to keep the solution in a static condition and with a fairly constant ionic composition [14, 34]. In contrast, Resende et al. [15] demonstrated that OCP can grow continuously for 28 days in static conditions with no ionic supply, i.e., without S-SBF refreshment. This result indicates that there are other factors involved during the deposition process. Lu

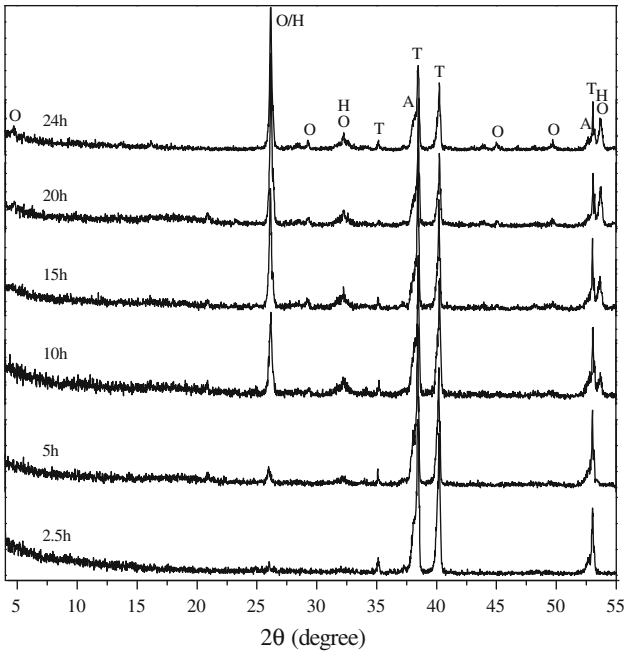

Fig. 10 XRD patterns of alkali and heat-treated titanium surfaces after immersion in S-SBF solution from 2.5 to 24 h. *T* titanium, *O* OCP, *H* HA and *A* anatase

and Leng [9] made a theoretical study of calcium phosphate precipitation in SBF solutions, analyzing the effect of interfacial energy on the nucleation rates of HA, OCP and dicalcium phosphate (DCPD). Their calculations showed that in physiological conditions the nucleation rate of OCP is always higher than that of HA, and the nucleation rate of DCPD is highest when DCPD precipitation is thermodynamically possible. Their findings are in agreement with those of Nelson et al. [37], who claimed that the nucleation of OCP is favored energetically because the surface energy of HA is higher than that of OCP. Another factor that might affect the OCP formation is the concentration of HCO_3^-. Lu and Leng [9] suggested that higher concentrations of HCO_3^- exclude apatite formation because nucleation of OCP is energetically more favorable than that of apatite in such conditions. Their analyses are based on the studies of Iijima [34], who demonstrated that in physiological environments, larger amounts of carbonate ions promote the nucleation of OCP instead of HA. Lu and Leng [9] used revised SBF solution, which contains large amounts of HCO_3^- (similar to that of human plasma), and detected OCP on bioactive titanium by electron diffraction. However, the solution used in this study has smaller amounts of HCO_3^- (identical to that of conventional SBF solution), and we found OCP. Moreover, it is well known that the use of conventional SBF solution leads to apatite formation on bioactive titanium. These results suggest that the driving force for OCP formation depends not only on the HCO_3^- concentration, but also on the other ions present in the solution. In fact, all the ions in the solution may play an important role in the kinetics of Ca–P phase formation and must be investigated in order to fully address this issue.

The kinetics of Ca–P deposition was evaluated by measuring the thickness of the coating after various periods of immersion in S-SBF solution. The thicknesses were measured by SEM and are presented in Fig. 13. The average values reveal a parabolic behavior typical of matter transport. It is more likely that the Ca–P deposition process is controlled by an interfacial reaction in the early period of the deposition and then by matter transport in the solution, i.e., by Ca–P diffusion in the aqueous solution. Figure 13 combined with Fig. 9 also emphasizes how rapid Ca/P deposition in S-SBF is compared with deposition in conventional SBF [15]. The formation of a uniform layer of apatite [15] in Kokubo solution takes at least 7–14 days, while a couple of hours in S-SBF solution suffices to form a homogeneous film of amorphous calcium phosphate and no more than 5 h to coat the titanium surface with an even layer of OCP. This means that S-SBF solution can radically reduce the time required to coat bioactive materials and represents a significant advance in the biomimetic-like deposition process. As can be seen in Fig. 13, the samples immersed in S-SBF for 2.5, 5 and 12.5 h had a thickness of approximately 1.8, 3.5 and 6.7 μm, respectively. Figure 14 is a representative SEM cross-section image of the coating obtained after immersion in S-SBF for 12.5 h. Note that the layer formed during the deposition process is bound to the substrate without forming a distinct interface. This suggests that the deposited Ca–P penetrates the pores of the underlying layers, rendering them more compact. Figure 4b indicates that the gel-like layer of ACP penetrated into the pores created by the NaOH attack.

4 Conclusions

This study contributes to a better understanding of the kinetics and mechanism of octacalcium phosphate deposition using a simplified simulated body fluid. The alkali and heat treatments produced a sodium titanate layer poorly crystallized. Heating also promoted the formation of crystalline anatase and rutile in the sodium titanate layer and at the interface with the metal. These changes on the titanium surface are suitable for Ca–P deposition in the simplified simulated body fluid solution, regardless of the formation of barium sodium titanate, which has no effect on the formation of the coating. This solution promotes rapid Ca–P deposition, resulting in a homogeneous plate-like film of OCP after 5 h of immersion. Calcium precipitates first, producing a thin layer of calcium titanate in the early stages of the deposition process. The process continues with the precipitation of calcium and phosphate

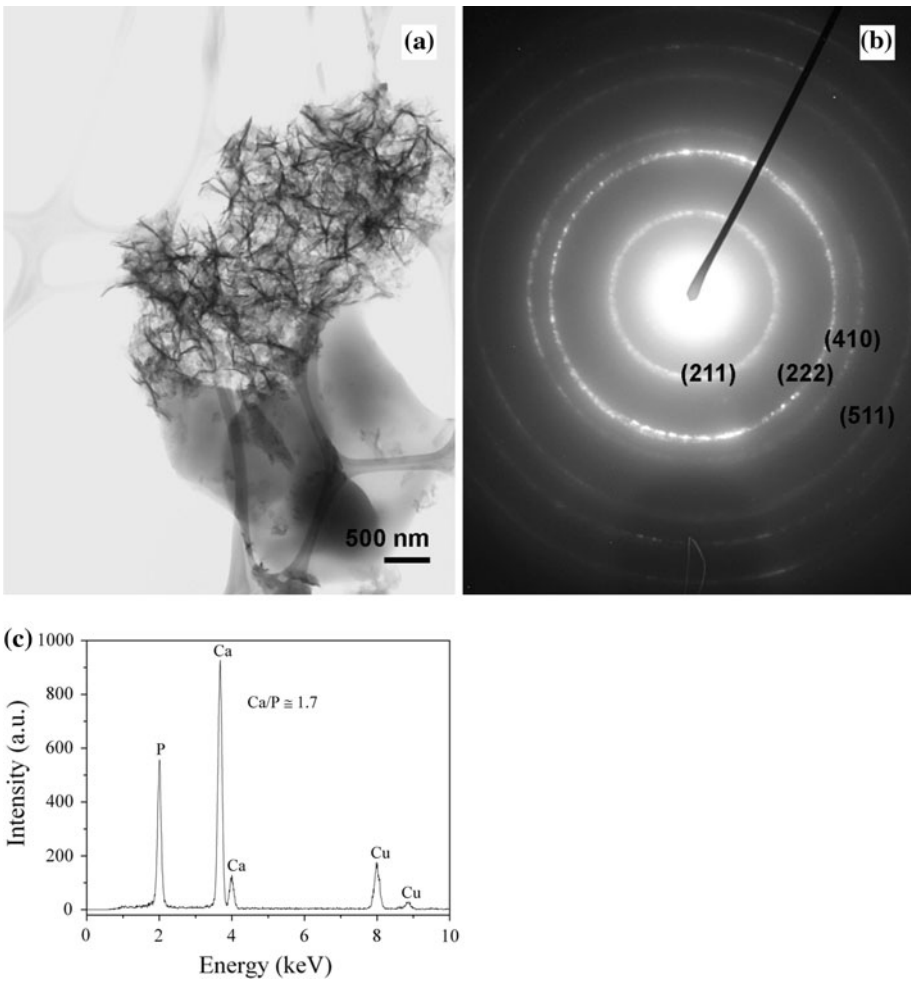

Fig. 11 TEM bright field image (**a**), diffraction pattern (**b**), and EDS spectrum (**c**) revealing the crystalline needle-like structure of HA of particles from the coating produced on titanium by immersion in S-SBF for 2.5 h. The HA particles are adjacent to an OCP plate

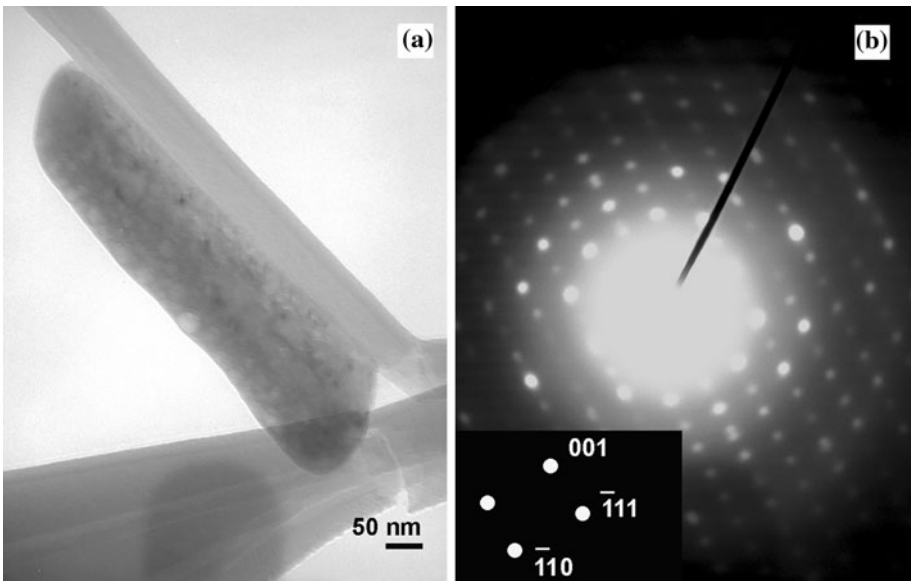

Fig. 12 TEM bright field image (**a**), and its diffraction pattern (**b**) of OCP from a titanium sample immersed in S-SBF for 6 h

on the calcium titanate film, promoting the formation of an amorphous calcium phosphate layer. After 2.5 h of immersion, the amorphous calcium phosphate layer showed OCP nuclei that grew continuously up to 24 h, forming regular and homogeneous plate-like crystals. Nucleation and growth of OCP occurred along with

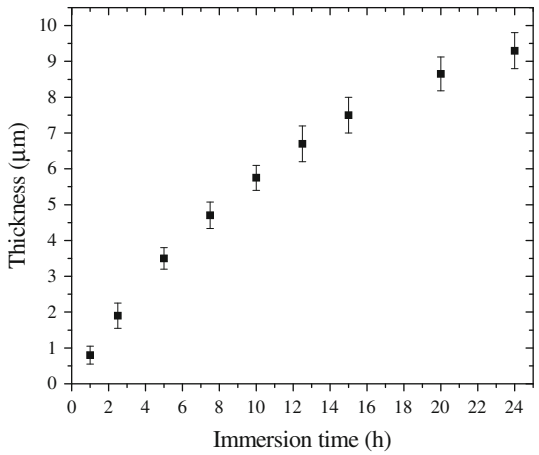

Fig. 13 Kinetics of Ca–P deposition on alkali and heat-treated titanium surfaces in S-SBF solution

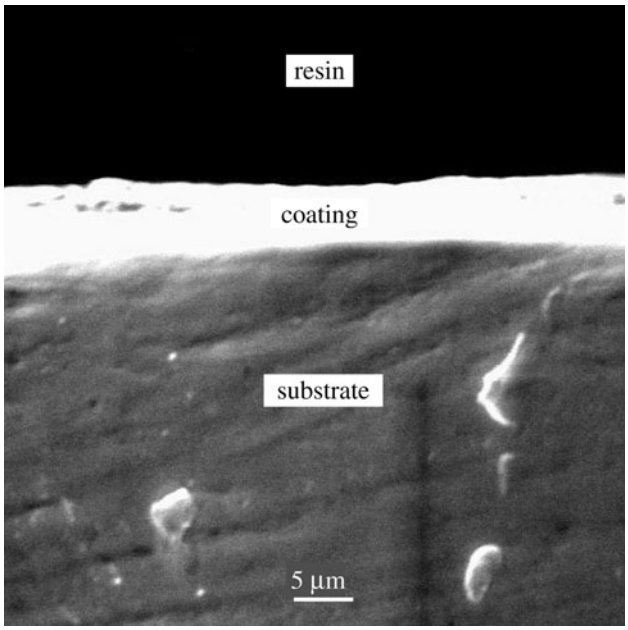

Fig. 14 SEM cross-section micrograph of alkali and heat-treated titanium sample showing the thickness of the coating after immersion in S-SBF for 12.5 h

crystallization of amorphous calcium phosphate into HA. This transformation occurred by solid-state diffusion and took place after approximately 1 h of immersion, forming islands of HA with a needle-like structure, which grew and crystallized in the transient amorphous calcium phosphate layer. The titanium surface was then essentially covered with an external layer of OCP and an intermediary layer of HA in contact with the OCP layer.

Acknowledgments The Brazilian research funding agencies CAPES, CNPq and FAPERJ are gratefully acknowledged for their financial support of this work.

References

1. Wu U, Ackerman JL, Strawich ES, Rey C, Kim H-M, Glimcher MJ. Phosphate ions in bone: identification of a calcium–organic phosphate complex by ^{31}P solid-state NMR spectroscopy at early stages of mineralization. Calcif Tissue Int. 2003;72:610–26.
2. Crane NJ, Popescu V, Moris MD, Steenhuis P, Ignelszi MA. Transient precursor strategy in mineral formation of bone. Bone. 2006;39:431–3.
3. R.Z. Legeros, Biological and synthetic apatites, in hydroxyapatite and related materials, edited by P.W. Brown and B. Constanz, CRC Press: Rocca-Batton; 1994. p. 3–28.
4. Brown WE, Eidelman N, Tomazic B. Octacalcium phosphate as a precursor in biomineral formation. Adv Dent Res. 1987;1:306–13.
5. Wen HB, Brink JVD, De Wijn JR, Cui FZ, De Groot K. Crystal growth of calcium phosphate on chemically treated titanium. J Cryst Growth. 1998;186:616–23.
6. Feng QL, Wang H, Cui FZ, Kim TN. Controlled crystal growth of calcium phosphate on titanium surface by NaOH-treatment. J Cryst Growth. 1999;200:550–7.
7. Li SJ, Yang R, Niinomi M, Hao YL, Cui YY. Formation and growth of calcium phosphate on the surface of oxidized Ti–29Nb–13Ta–4.6Zr alloy. Biomaterials. 2004;25:2525–32.
8. Lu X, Zhao Z, Leng Y. Biomimetic calcium phosphate coatings on nitric-acid-treated titanium surfaces. Mater Sci Eng C. 2007;27:700–8.
9. Lu X, Leng Y. Theoretical analysis of calcium phosphate precipitation in simulated body fluid. Biomaterials. 2005;26:1097–108.
10. Wu W, Nancollas GH. Kinetics of heterogeneous nucleation of calcium phosphates on anatase and rutile surfaces. J Colloid Inter Sci. 1998;199:206–11.
11. Xie Y, Liu X, Chu PK, Ding C. Nucleation and growth of calcium–phosphate on Ca-implanted titanium surface. Surf Sci. 2006;600:651–6.
12. Barrère F, Van Blitterswijk CA, De Groot K, Layrolle P. Influence of ionic strength and carbonate on the Ca–P coating formation from SBFx5 solution. Biomaterials. 2002;23:1921–30.
13. Jonášová L, Müller FA, Helebrant A, Strnad J, Greil P. Biomimetic apatite formation on chemically treated titanium. Biomaterials. 2004;25:1187–94.
14. Lu X, Leng Y. TEM study of calcium phosphate precipitation on bioactive titanium surfaces. Biomaterials. 2004;25:1779–86.
15. Resende CX, Dille J, Platt GM, Bastos IN, Soares GA. Characterization of coating produced on titanium surface by a designed solution containing calcium and phosphate ions. Mater Chem Phys. 2008;109:429–35.
16. Xiao X-F, Tian T, Liu R-F, De She H. Influence of titania nanotube arrays on biomimetic deposition apatite on titanium by alkali treatment. Mater Chem Phys. 2007;106:27–32.
17. Oh S-H, Finõnes RR, Daraio C, Chen L-H, Jin S. Growth of nano-scale hydroxyapatite using chemically treated titanium oxide nanotubes. Biomaterials. 2005;26:4938–43.
18. Kamakura S, Sasano Y, Suzuki O. Synthetic octacalcium phosphate (OCP) in an effective scaffold to regenerate bone. Inter Congress Series. 2005;1284:290–5.
19. Heughebaert J-C, Zawacki SJ, Nancollas GH. The growth of octacalcium phosphate on beta tricalcium phosphate. J Cryst Growth. 1983;63:83–90.
20. Morris HF, Ochi S, Spray JR, Olson JW. Periodontal-type measurements associated with hydroxyapatite-coated and non—HA-coated implants: uncovering to 36 months. Ann Periodontal. 2000;5:56–67.
21. Geurs NC, Jeffcoat RL, McGlumphy EA, Reddy MS, Jeffcoat MK. Influence of implant geometry and surface characteristics on

progressive osseointegration. Int J Oral Maxillofac Implants. 2002;17:811–5.
22. I.N. Bastos, G.M. Platt, G.D. De Almeida Soares, Thermodynamics study of simplified SBF solutions, Proceedings of 18th International Congress of Mechanical Engineering, November 6–11, CDROM, Brazil:Ouro Preto-MG; 2004.
23. Chen Y, Zheng X, Ji H, Ding C. Effect of Ti–OH formation on bioactivity of vacuum plasma-sprayed titanium coating after chemical treatment. Surf Coat Tech. 2007;202:494–8.
24. Feng QL, Cui FZ, Wang H, Kim TN, Kim JO. Influence of solution conditions on deposition of calcium phosphate on titanium by NaOH-treatment. J Cryst Growth. 2000;210:735–40.
25. Feng B, Weng J, Yang BC, Chen JY, Zhao JZ, He L, Qi SK, Zhang XD. Surface characterization of titanium and adsorption of bovine serum albumin. Mater Charac. 2003;49:129–37.
26. Cheng X, Roscae SG. Corrosion behavior of titanium in the presence of calcium phosphate and serum proteins. Biomaterials. 2005;26:7350–6.
27. Pouilleau J, Devilliers D, Garrido F, Durand-vidal S, Mahe E. Structure and composition of passive titanium oxide films. Mater Sci Eng. 1997;B47:235–43.
28. Kokubo T, Matsushita T, Takadama H. Titania-based bioactive materials. J Eur Cer Soc. 2007;27:1553–8.
29. Liang F, Zhou L, Wang K. Apatite formation on porous titanium by alkali and heat-treatment. Surf Coat Tech. 2003;165:133–9.
30. Xue W, Liu X, Zheng XB, Ding C. In vivo evaluation of plasma-sprayed titanium coating after alkali modification. Biomaterials. 2005;26:3029–37.
31. Zhang Q, Leng Y, Xin R. A comparative study of electrochemical deposition and biomimetic deposition of calcium phosphate on porous titanium. Biomaterials. 2005;26:2857–65.
32. Lu X, Zhao Z, Leng Y. Calcium phosphate crystal growth under controlled atmosphere in electrochemical deposition. J Cryst Growth. 2005;284:506–16.
33. Takadama H, Kim HM, Kokubo T, Nakamura T. TEM-EDX study of mechanism of bone-like apatite formation on bioactive titanium metal in simulated body fluid. J Biomed Mater Res. 2001;57:441–8.
34. Iijima M. Growth and structure of lamellar mixed crystals of octacalcium phosphate and apatite in a model system of enamel formation. J Cryst Growth. 1992;116:319–26.
35. Marques PAAP, Magalhães MCF, Correia RN. Inorganic plasma with physiological CO_2/HCO_3 buffer. Biomaterials. 2003;24:1541–8.
36. Leng Y, Chen J, Qu S. TEM study of calcium phosphate precipitation on HA/TCP ceramics. Biomaterials. 2003;24:2125–31.
37. Nelson DGA, Barry JC, Shields CP, Glena R, Featherstone JDB. Crystal morphology, composition, and dissolution behavior of carbonated apatites prepared and controlled pH and temperature. J Colloid Inter Sci. 1989;130:467–79.